Polymer-Induced Structural Transitions in Oleate Solutions: Microscopy, Rheology, and Nuclear Magnetic Resonance Studies

Zuchen Lin* and Charles D. Eads

Miami Valley Laboratories, The Procter & Gamble Company, P.O. Box 538707, Cincinnati, Ohio 45253-8707

Received October 17, 1996. In Final Form: February 20, 1997[⊗]

Cryo-transmission electron microscopy (cryo-TEM), NMR, and rheometry were used to study polymer/surfactant interactions involving the nonionic polymers polyethylene glycol (PEG) and polypropylene glycol (PPG) and the surfactant potassium oleate in aqueous solution. In the absence of polymer, the surfactant solution was viscoelastic. Cryo-TEM showed that the surfactant formed threadlike micelles and NMR diffusion measurements also indicated a large micelle size. These micelles are similar to those formed by cationic alkyltrimethylammonium halides. Addition of PEG or PPG induced a viscoelastic-to-Newtonian liquid transition. In contrast to the behavior seen with the cationic surfactants, PEG is more effective than the more hydrophobic polymer, PPG, in inducing this transition. Cryo-TEM images showed a threadlike-to-spherical micelle transition in these polymer/surfactant systems. The extent of the threadlike-to-spherical transition detected by cryo-TEM for PEG compared to PPG correlates with the effectiveness of the two polymers in influencing solution rheology. Self-diffusion coefficients determined by NMR support an association between the surfactant and either polymer and a greatly reduced micellar hydrodynamic radius for the surfactant/polymer complex. The increase in surfactant diffusion coefficient caused by PEG compared to PPG also correlates with the effectiveness of the two polymers in influencing solution rheology. Two-dimensional nuclear Overhauser effect spectroscopy demonstrated a close proximity and long-lived interaction between oleate and PEG in the complex and suggests that all surfactant atoms have a measurable probability of being close to the polymer. The NMR data also established that internal aggregate dynamics are in the spin-diffusion (slow) limit.

Introduction

Polymers and surfactants are commonly found in many commercial products. Surfactants are characterized by the presence of two moieties in the same molecule, one polar and the other nonpolar. The existence of groups with opposing characteristics is responsible for all the special properties of surfactants. The behavior of surfactants in aqueous solution is determined by their tendency to seclude their hydrophobic part and expose their hydrophilic part toward the solvent. Polymers can interact with surfactants and change the surfactant microstructures, thereby altering microscopic and macroscopic properties of the system. We may consider the interaction either in terms of the binding of surfactant molecules to a polymer molecule or in terms of the effect of the polymer chains on surfactant self-assembly.[1]

Since Jones'[2] pioneering work on properties of a mixed polyethylene oxide (PEG)/sodium dodecyl sulfate (SDS) system, complex formation between surfactants and polymers has been the subject of intensive research,[3−11] leading to significant progress toward understanding polymer−surfactant complex formation.[12] Nonionic polymers and anionic surfactants are the most investigated polymer−surfactant systems. The association of polyethylene glycol (PEG) with sodium dodecyl sulfate (SDS) has been extensively studied by a variety of techniques.[2−12] Polymer−surfactant aggregates are generally visualized as polymer molecules wrapped around the exposed, hydrophilic surface of surfactant aggregates at the aqueous interface. Theoretical work has been guided by thermodynamic considerations to explain the nature of complexation of nonionic polymer molecules with surfactant aggregates such as globular micelles, rodlike micelles, bilayers, and microemulsions.[13−15] Formation of the complexes is attributed to three major factors: favorable enhanced shielding of the hydrophobic core from water, unfavorable increased steric repulsion at the aggregate surface, and favorable hydrophobic interaction between nonpolar polymer moieties and surfactant molecules. The magnitude of the last factor depends on the hydrophobicity of the polymer. These factors have been used to explain polymer-induced microstructural changes in cationic and nonionic surfactant solutions.[16] In particular, a threadlike-to-spherical micelle transition was found in cetyltrimethylammounium bromide (CTAB)/sodium salicylate (NaSal) solution with addition of nonionic polymers, such as poly(vinyl methyl ether) (PVME) and polypro-

[⊗] Abstract published in *Advance ACS Abstracts,* April 15, 1997.

(1) Lindman, B.; Thalberg, K., Polymer−surfactant interactions−recent developments. In *Interactions of Surfactants with Polymers and Proteins;* Goddard, E. D., Anathapadmanabham, K. P., Eds.; CRC Press: Boca Raton, FL, 1993; pp 203−276.
(2) Jones, M. N. *J. Colloid Interface Sci.* **1967**, *23*, 36−42.
(3) Moroi, Y.; Akisada, H.; Saito, M.; Matuura, R. *J. Colloid Interface Sci.* **1977**, *61*, 233−238.
(4) Shirahama, K.; Tohdo, M.; Murahashi, M. *J. Colloid Interface Sci.* **1982**, *86*, 282−283.
(5) Brackman, J. C.; Engberts, J. B. F. N. *J. Colloid Interface Sci.* **1989**, *132*, 250−255.
(6) Brown, W.; Fundin, J.; Miguel, M. da G. *Macromolecules* **1992**, *25*, 7192−7198.
(7) Quina, F.; Abuin, E.; Lissi, E. *Macromolecules* **1990**, *23*, 5173−5175.
(8) Turro, N. J.; Baretz, B. H.; Kuo, P.-L. *Macromolecules* **1984**, *17*, 1324−1331.
(9) Maltesh, C.; Somasundaran, P. *Langmuir* **1992**, *8*, 1926−1930.
(10) Ruckenstein, E.; Huber, G.; Hoffman, H. *Langmuir* **1987**, *3*, 382−387.
(11) Dubin, P. L.; Gruber, J. H.; Xia, J.; Zhang, H. *J. Colloid Interface Sci.* **1992**, *148*, 35−41.
(12) Goddard, E. D., Anathapadmanabham, K. P., Eds. *Interactions of Surfactants with Polymers and Proteins;* CRC Press: Boca Raton, FL, 1993.
(13) Nagarajan, R. *Colloids Surf.* **1985**, *13*, 1−17.
(14) Nagarajan, R. *J. Chem. Phys.* **1989**, *90*, 1980−1994.
(15) Ruckenstein, E.; Huber, G.; Hoffman, H. *Langmuir* **1988**, *3*, 382−287.
(16) Li, X.; Lin, Z.; Cai, J.; Davis, H. T.; Scriven, L. E. *J. Phys. Chem.* **1995**, *99*, 10865−10878.

S0743-7463(96)01004-9 CCC: $14.00

pylene glycol (PPG).[16−18] It has also been found that PEG does not have appreciable interaction with CTAB micelles.[17] The fact that PEG is not as hydrophobic as PVME and PPG was used to explain the difference in interacting with CTAB micelles. This is consistent with theories in which sufficient hydrophobicity of the polymer is required. In addition, a study of the interactions between hydrophobically-modified water-soluble polymers and surfactants revealed the different interactions between polymer−micelle and polymer−bilayer.[19]

It has been found that anionic surfactants interact more strongly than cationic ones with nonionic polymers. Several theories have been developed to explain the differences between them. The most popular one is that the large head groups (such as trimethylammonium group) typical of cationic surfactants will reduce the access of the polymer to the surface of the micelles.[13−15] It has been reported that dodecylammonium chloride interacts more strongly than dodecylpyridinium chloride with polymer.[20] However, the size of the head group may not be the only factor. Witte and Engberts[21] also suggested that there is a difference in interactions of cations and anions with the hydration shell of the polymer, which would favor the interaction of anionic surfactants. They also found that PPG interacts more strongly with SDS micelles than does PEG.

In this paper, rheometry, cryo-transmission electron microscopy (cryo-TEM), and nuclear magnetic resonance (NMR) are used to investigate the interactions between oleate soap and the nonionic polymers PEG and PPG in aqueous solution. Rheometry demonstrates a viscoelastic-to-Newtonian liquid transition upon the addition of these polymers to oleate soap. The structural basis for this transition is shown by cryo-TEM to be a change in aggregate structure from threadlike to spherical micelles, while NMR shows corresponding changes in aggregate size.

Materials and Methods

Materials. Oleic acid, polyethylene glycol (PEG-8000, MW = 8000, and PEG-4600, MW = 4600), and polypropylene glycol (PPG-4000, MW = 4000) were purchased from Sigma Chemical Co. (St. Louis, MO) and used without further purification. All other materials were used as obtained from standard suppliers.

The pH was about 12 in all samples used in cryo-TEM and rheology studies. For cryo-TEM and rheology studies, the oleic acid concentration was kept at 2.65%. Potassium hydroxide and a small amount (0.65%) of sodium bicarbonate were added to bring the pH to about 12. For NMR studies, dibasic potassium carbonate was present at 7% and the polymer and surfactant concentrations are given in the figure legends. The pH was above 11 for all NMR samples.

Cryo-TEM. Cryo-TEM samples were prepared in the controlled environment vitrification system (CEVS).[22] A 5-μL drop of the sample solution was placed on a carbon-coated holey polymer support film which was mounted on the surface of a standard 300-mesh TEM grid (from Ted Pella, catalog no. 01883-F). The drop was blotted with filter paper until it was reduced to a thin film (10−200 nm) spanning the holes (2−10 μm) in the support film. The sample was then vitrified by rapidly plunging it through a synchronous shutter at the bottom of the CEVS into liquid ethane at its freezing point. The vitreous specimen was transferred under liquid nitrogen to the cryo-TEM transfer stage (Model 626, Gatan Inc., PA), which was inserted into the microscope (Philips CM12, Mahwah, NJ) for *direct* observation. The temperature was maintained below −170 °C throughout specimen observation. The specimen was imaged at 100 kV and an underfocus of 2−4 μm in order to achieve the phase contrast responsible for image contrast formation. The images were recorded on Kodak SO-163 films that were developed with full-strength D-19 developer (Eastman Kodak Co., Rochester, NY) for 12 min.

Rheology. Steady shear and small-amplitude oscillatory shear, i.e., dynamic shear, were performed on a Rheometrics Dynamic Stress Rheometer SR500, which is supported by RHIOS software. Dynamic shear measurements were taken over the frequency sweep from 0.1 to 100. The rheometer has a built-in computer which converts the torque measurements into both G' (the storage modulus) and G'' (the loss modulus) in dynamic shear experiments or viscosity in steady shear experiments. The dynamic shear measurement was carried out in Couette or concentric cylinder geometry, the cup radius was 17 mm, and the bob radius and length were 16 mm and 33 mm, respectively. All tests were done at room temperature.

NMR. All NMR measurements were performed using a GE Omega 500 MHz NMR spectrometer equipped with an S-17 gradient probe accessory. Diffusion coefficients were determined using the stimulated-echo pulse sequence.[23] During each measurement, delays were kept constant and the residual signal intensity was measured as a function of gradient strength. Diffusion coefficients were extracted from the data by fitting to the Stejskal-Tanner equation[24] using fitting software provided with the spectrometer. Gradient strength was calibrated to give a diffusion coefficient for residual HOD in D_2O of 1.902×10^{-7} cm^2 s^{-1} [25] and was approximately 30 G/cm at 5 A. Sample temperature was controlled to ± 0.1 °C using the apparatus supplied with the spectrometer.

Phase-sensitive, two-dimensional nuclear Overhauser effect spectroscopy (NOESY)[26] was performed using the standard three-pulse sequence. Quadrature detection in t1 was achieved using the TPPI method.[27] A gradient pulse was used during the mixing time to remove signal arising from undesired coherence transfer pathways. An eight-step phase cycle was used to remove axial peaks and quadrature artifacts and to further suppress undesired coherence transfer pathways. Typical spectra had 1K complex points in t2, and 512 t1 increments. Spectra were processed and peak volumes were integrated using commercial software (Felix 2.30, Biosym, Inc.).

Results

Figure 1 shows a cryo-TEM image of the oleate solution without any polymer. Long, entangled threadlike micelles are evident. These structures can account for the viscoelasticity of the solution. It is difficult to measure the micellar length because one cannot trace one single micelle from end to end, but the structures are at least 0.1 μm in length.

In the absence of polymer, the oleate solution exhibits strong viscoelasticity and shear thinning behavior. Dynamic oscillatory measurements showed a large elastic modulus G' (Figure 2), which decreased rapidly with the decrease of frequency. The crossover of G' and G'' is at about 0.075 1/s, indicating a long relaxation time for the system. A simple Maxwell element was used to analyze the data. However, the Maxwell model does not fit the data, indicating there is more than one relaxation time associated with the system.

Figure 3 displays the steady-state shear viscosity measurement. The solution showed a strong shear

(17) Brackman, J. C.; Engberts, J. B. F. N. *Langmuir* **1991**, *7*, 2097−2102.
(18) Brackman, J. C.; Engberts, J. B. F. N. *Chem. Soc. Rev.* **1993**, *22*, 85.
(19) Kevelam, J.; van Breemen, J. F. L.; Blokzijl, W.; Engberts, J. B. F. N. *Langmuir* **1996**, *12*, 4709−4717.
(20) Shirahama, K.; Oh-Ishi, M.; Takisawa, N. *Colloids Surf.* **1989**, *40*, 261.
(21) Witte, F. M.; Engberts, J. B. F. N. *Colloids Surf.* **1989**, *36*, 417.
(22) Bellare, J. R.; Davis, H. T.; Scriven, L. E.; Talmon, Y. *J. Electron Microsc. Tech.* **1988**, *10*, 87−111.
(23) Tanner, J. E. *J. Chem. Phys.* **1970**, *52*, 2523−2526.
(24) Stejskal, E. O.; Tanner, J. E. *J. Chem. Phys.* **1965**, *42*, 288−292.
(25) Holz, M.; Weingärtner, H. *J. Magn. Reson.* **1991**, *92*, 115−125.
(26) Macura, S.; Ernst, R. R. *Molecular Physics* **1980**, *41*, 95−117.
(27) Marion, D.; Wüthrich, K. *Biochem. Biophys. Res. Commun.* **1980**, *113*, 967−974.

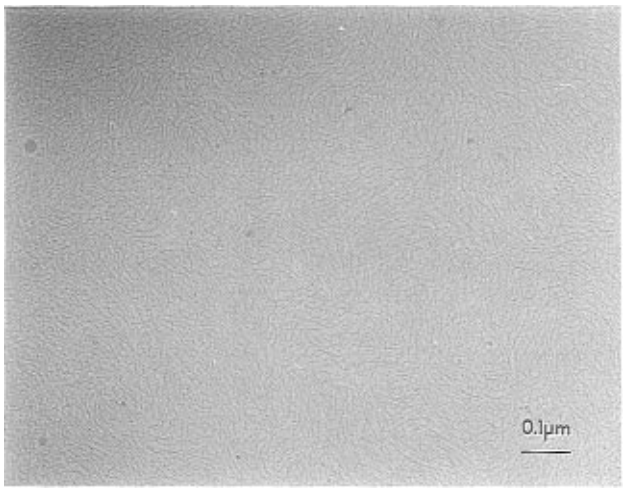

Figure 1. Cryo-TEM image of an oleate solution. The sample contained 2.65% oleic acid and 0.65% $NaHCO_3$ in H_2O. Long, entangled thread like micelles were found.

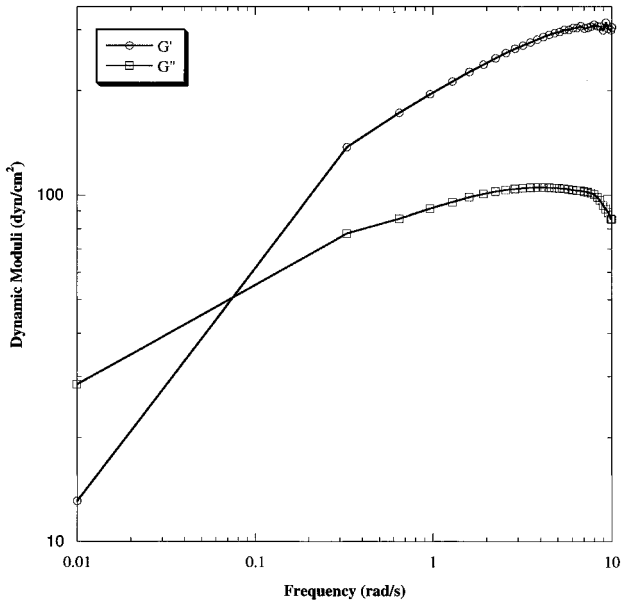

Figure 2. Dynamic oscillatory measurement for an oleate solution. The sample contained 2.65% oleic acid and 0.65% $NaHCO_3$ in H_2O. A simple Maxwell model cannot fit the data.

thinning effect. Unlike some branched micellar systems,[28] the plot of shear rate against applied shear stress (Figure 4) showed the system does not have a yield stress value.

With addition of polymer, the solution viscosity dropped 2 decades. The steady-state shear viscosity measurement also showed that solutions became Newtonian liquids (Figure 5) with either PEG or PPG.

By comparing viscosities of solutions with PEG to those of solutions with PPG at equal polymer concentrations, one can conclude that PEG is more effective in viscosity reduction than PPG. This is opposite to previous studies on polymer−cetyltrimethylammonium bromide (CTAB)/sodium salicylate (NaSal) systems, wherein more hydrophobic polymers, such as poly(vinyl methyl either) (PVME) and PPG, were more effective than hydrophilic polymers in viscosity reduction.[16,17]

Figure 6 shows a cryo-TEM image of an oleate solution with addition of 0.5% PPG. Although the system still consists of threadlike micelles, the micellar length appeared shorter compared to the polymer-free sample (Figure 1), as one can find more ends from the micrograph.

(28) Lin, Z. *Langmuir* **1996**, *12*, 1729−1737.

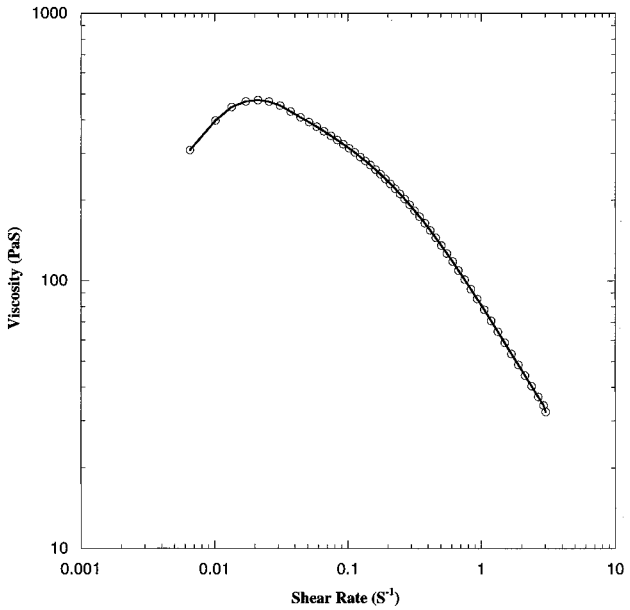

Figure 3. Steady-state shear viscosity measurement of an oleate solution. The samples contained 2.65% oleic acid and 0.65% $NaHCO_3$ in H_2O.

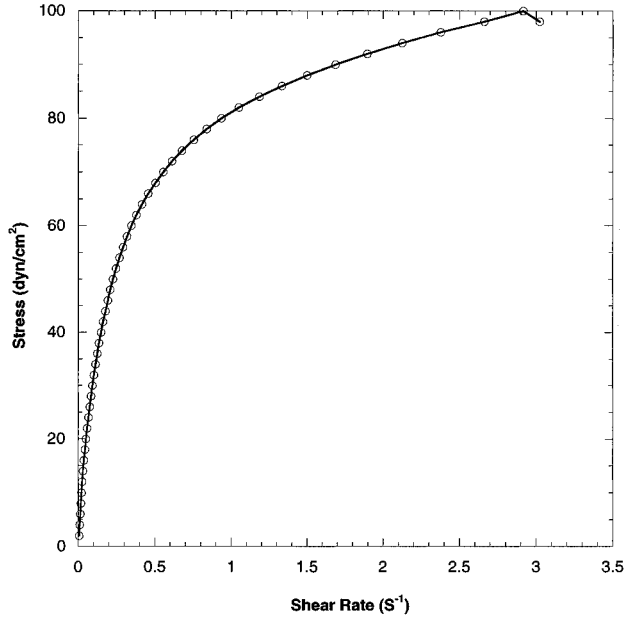

Figure 4. Shear rate dependence of shear stress for an oleate solution. The samples contained 2.65% oleic acid and 0.65% $NaHCO_3$ in H_2O. No yield stress value was found.

Figure 7 displays a cryo-TEM image of an oleate solution with addition of 1% PPG. It showed disentanglement of micelles and a further reduction of micelle length. Figures 8and 9 show cryo-TEM images of oleate solutions with 0.5% and 1% PEG, respectively. The solutions with PEG follow the same trend as those with PPG. However, PEG is more effective in reducing micelle length. Only spherical micelles were found in 1% PEG/oleate solution, indicating a threadlike-to-spherical micelle transition occurred in the system. This transition has also been found in the CTAB/NaSal system with addition of more hydrophobic polymers, such as PVME or PPG.[16−18] These structural changes clearly underlie the viscosity reduction and the non-Newtonian-to-Newtonian fluid transition. When the solution has only spherical micelles, it has low viscosity and exhibits Newtonian behavior.

Figure 10 shows diffusion coefficients determined by NMR as a function of temperature for PEG-8000 and oleate

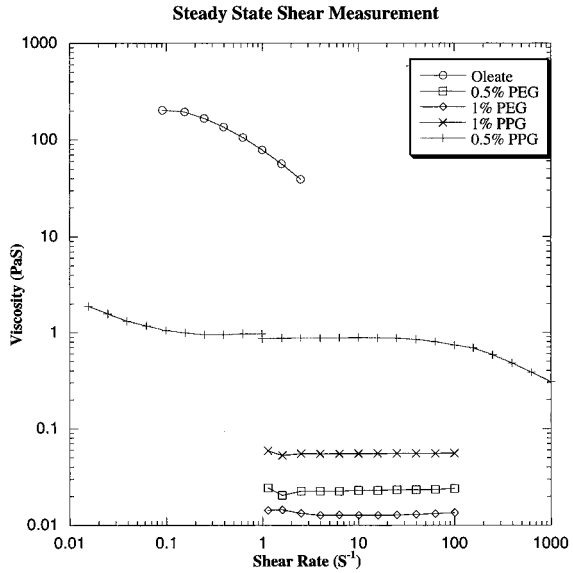

Figure 5. Steady-state shear viscosity measurements of oleate−polymer solutions. The samples contained 2.65% oleic acid, 0.65% $NaHCO_3$, and different levels of PEG-8000 and PPG-4000 in H_2O. The oleate sample without polymer is also included for comparison.

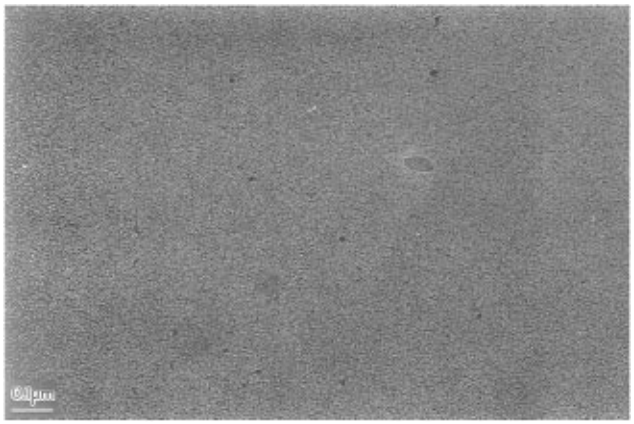

Figure 6. Cryo-TEM image of an oleate-polymer solution. The sample contained 2.65% oleic acid, 0.65% $NaHCO_3$, and 0.5% PPG-4000 in H_2O. Threadlike micelles still dominate.

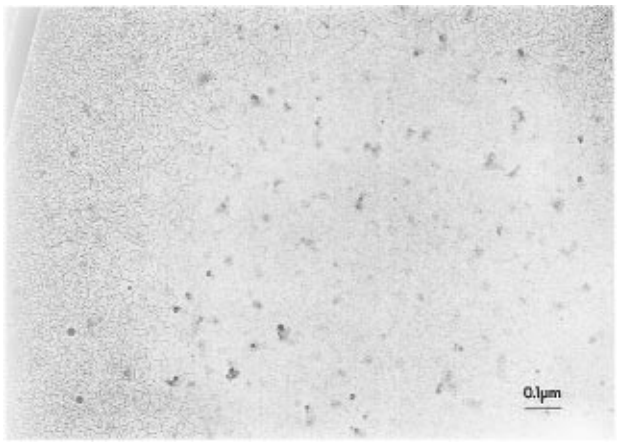

Figure 7. Cryo-TEM image of an oleate−polymer solution. The sample contained 2.65% oleic acid, 0.65% $NaHCO_3$, and 1% PPG-4000 in H_2O. Short, threadlike micelles dominate. A few spherical micelles can be found.

separately in different solutions and together in the same solution. The diffusion rate of PEG alone is much faster than the diffusion rate of oleate alone. For the oleate, the diffusion coefficient corresponds to an effective hydrodynamic radius of approximately 3000 Å at the highest temperature. This is unlikely to correspond to a true dimension of the aggregates but does illustrate the large aggregate size and hindered diffusion. The diffusion coefficient of residual HOD in the oleate-containing samples was altered little by the presence of the surfactant

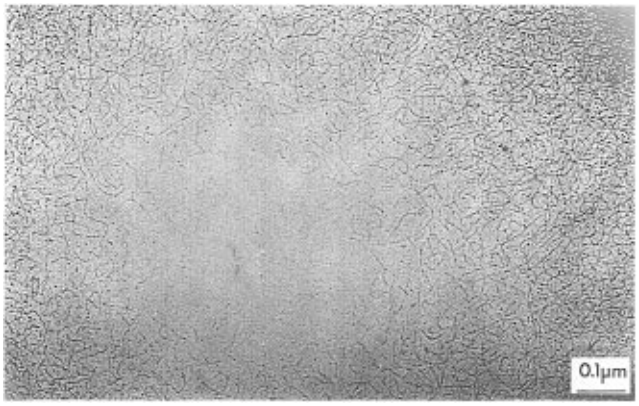

Figure 8. Cryo-TEM image of an oleate−polymer solution. The sample contained 2.65% oleic acid, 0.65% $NaHCO_3$, and 0.5% PEG-8000 in H_2O. Short, threadlike micelles and a few spherical micelles were found.

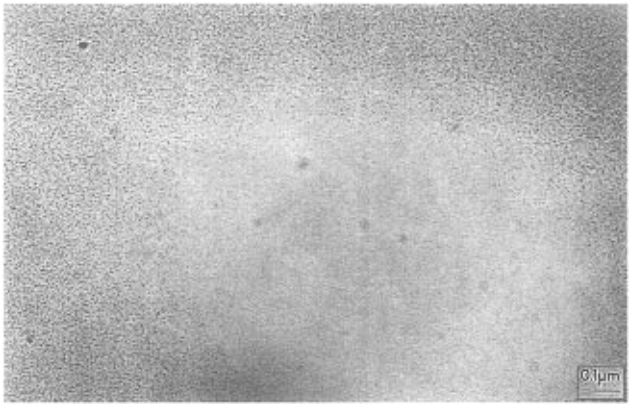

Figure 9. Cryo-TEM image of an oleate−polymer solution. The sample contained 2.65% oleic acid, 0.65% $NaHCO_3$, and 1% PEG-8000 in H_2O. Only spherical micelles were found in solution.

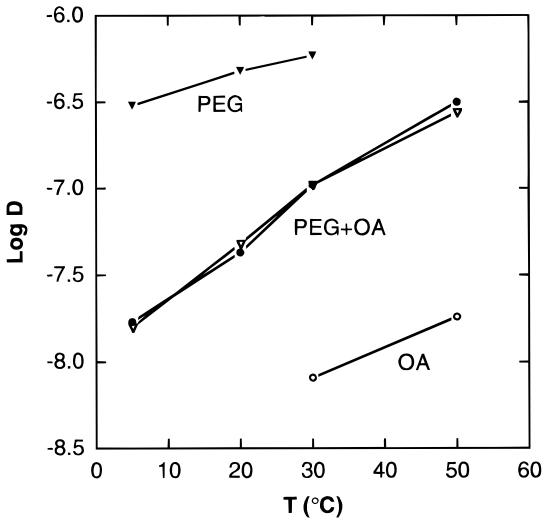

Figure 10. Temperature dependence of diffusion coefficients for oleate and PEG in different and in the same solution. Diffusion coefficients are in units of $cm^2\ s^{-1}$. Oleic acid-containing samples contained 2.8% oleic acid, 1.5% KOH, and 0.68% $NaHCO_3$ in D_2O. PEG-8000 was present at 0.5% in polymer-containing samples.

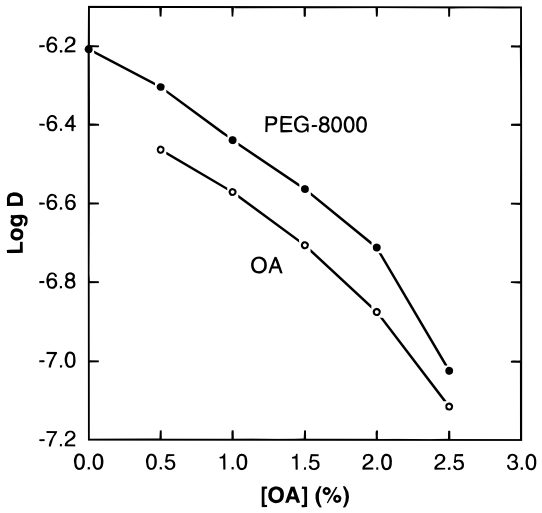

Figure 11. Surfactant dependence of polymer and surfactant diffusion coefficients at fixed (1%) PEG-8000 concentration. Diffusion coefficients are in units of $cm^2\ s^{-1}$. Solutions contained 1% PEG-8000, 7% K_2CO_3, and variable oleate.

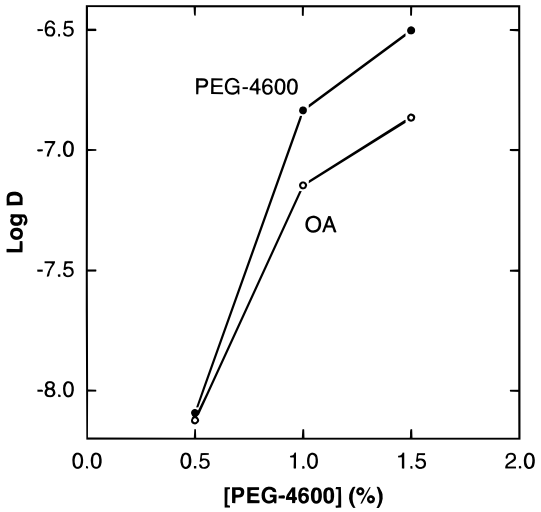

Figure 12. Polymer dependence of polymer and surfactant diffusion coefficients at fixed (2.5%) oleate concentration. Diffusion coefficients are in units of $cm^2\ s^{-1}$. Solutions contained 2.5% oleic acid, 7% K_2CO_3, and variable PEG-4600.

(data not shown). This demonstrates that water mobility is not restricted by large aggregates,[29] though such restriction would not be expected at the low surfactant concentrations used. When combined under the conditions of this experiment in which the ratio of polymer to surfactant is relatively low (see below), the polymer and surfactant diffuse with nearly identical rates, indicating a tight association. The effective hydrodynamic radius of the oleate−PEG complex is temperature dependent, decreasing from 850 Å at 5 °C to 150 Å at 50° C. These results demonstrate that the oleate and PEG associate to form aggregates of greatly reduced size and that at higher temperatures the aggregates break apart into smaller pieces. This polymer−surfactant association and reduction in aggregate size correlate with the reduction of solution viscosity demonstrated in rheology measurements. The effective hydrodynamic radii also correlate roughly with the cryo-TEM images acquired under similar conditions (Figure 8).

To explore the effects on aggregate behavior of polymer size and relative concentrations of polymer and surfactant, diffusion coefficients were measured for a system with the PEG-8000 concentration fixed at 1% and variable oleate or with oleate fixed at 2.5% and variable PEG-4600 concentration. Figure 11 shows that for a fixed concentration of PEG, a steady decrease in the diffusion coefficient of both components results from an increase in the surfactant concentration. Over the range of concentrations studied, the polymer diffuses about 40% more rapidly than the surfactant, although the difference narrows at higher oleate concentrations. Figure 12 shows that for a fixed concentration of oleate, increasing the concentration of PEG causes an increase in the diffusion coefficient for both components. At the lowest concentration of polymer, the two components diffuse with similar diffusion coefficients, as observed for the system studied in Figure 10. At the highest polymer concentration, the diffusion coefficient of the polymer exceeds that of the surfactant by more than a factor of 2. Diffusion coefficients can be compared for the two different polymer molecular weights of 8000 and 4600 for the samples containing identical weight fractions of 2.5% oleate and 1% polymer. For PEG, the ratio of diffusion coefficients for the high and low molecular weight systems is 0.65, while for oleate the corresponding ratio is 1.08. Thus, for the same number of oxyethylene units, the higher molecular weight polymer produces a smaller diffusion coefficient for the polymer while the diffusion coefficient for the surfactant is slightly increased.

To examine the role of polymer hydrophobicity, a sample was prepared with 2.5% oleate and 1% polymer, with the PEG replaced with PPG-4000. This can be directly compared to a similar sample containing identical concentrations of oleate and polymer (PEG) and with a similar polymer molecular weight. The diffusion coefficients determined for this system are 8.87×10^{-9} cm^2/s for PPG and 1.72×10^{-8} cm^2/s for oleate. Compared to the PEG system of comparable molecular weight and identical concentrations, the diffusion coefficients for the PPG system are reduced 16-fold and 4-fold for the polymer and surfactant, respectively. In contrast to PEG, the PPG diffusion coefficient is smaller than that of the surfactant. PPG therefore has a smaller effect on the size of the surfactant aggregate. Explaining the observation that the PPG diffuses more slowly than oleate will require additional investigation. It should be noted that PPG is not soluble at these concentrations in the absence of surfactant and self-aggregation of PPG may be influencing the results.

Two-dimensional nuclear Overhauser effect spectroscopy (NOESY) was also used to study the oleate/PEG system. Figure 13 shows an example of NOESY spectrum of the oleate/PEG system. Cross peaks are observed between PEG and all resolvable oleate resonances. Cross peaks are also observed among nearly all pairs of resolvable oleate resonances. In NOESY spectra, observation of cross peaks between molecules demonstrates that the two molecules are in close proximity (≤5 Å) for a significant fraction of the time. Thus, the cross peaks joining PEG and oleate atoms demonstrate that the oleate and PEG have formed a complex. The sign of the cross peaks contains information about the dynamics of the interaction between the corresponding atoms. When the sign of the cross peak is the same as that of the diagonal, the correlation time τ_c for the interaction is long compared to the inverse of the spectrometer frequency ω. This places a lower limit on the lifetime of the surfactant/polymer complex of $\tau_c \gg 1/\omega$. The sign of the cross peaks among the oleate atoms also reflects the rate of motion of oleate molecules within the aggregate. A NOESY spectrum of

(29) Lindman, B.; Olsson, U.; Söderman, O. In *Dynamics of Solutions and Fluid Mixtures by NMR*; Delpeuch, J. J., Ed.; John Wiley & Sons, Ltd.: New York, 1995; pp 345−395.

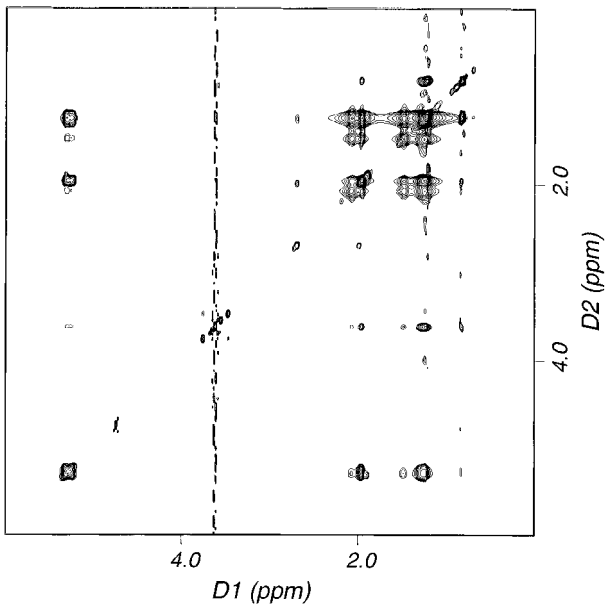

Figure 13. NOESY spectrum of complex of oleate with PEG. Sample contained 1.5% PEG-8000, 2.5% oleate, and 7% K_2CO_3 in D_2O. A mixing time of 400 ms was used. The horizontal band of peaks near 3.6 ppm corresponds to cross peaks joining oleate resonance with the polymer.

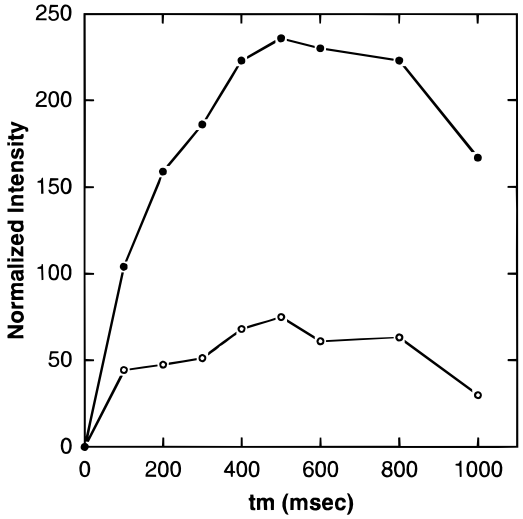

Figure 14. Cross-peak build-up curves for NOESY spectra of oleate−PEG complex. The sample composition is described in the legend to Figure 10. The filled circles represent the large group of unresolvable methylene resonances (positions 4−7 and 12−17), while the open circles represent the terminal methyl group (position 18). These two signals represent the largest and smallest build-up rates, respectively. The intensity is in arbitrary units, normalized to the number of hydrogen atoms contributing to the signal.

neat oleic acid was acquired to provide a comparison for the dynamics. This showed no observable cross peaks (data not shown), indicating that for the neat system, $\tau_c \leq 1/\omega$. Thus, motions of oleate molecules within the aggregates are slow compared to motions in the neat oleic acid.

To quantitate the relative intensities of oleate-PEG cross peaks in the NOESY spectrum, cross peak build-up rates were determined by examining the dependence of the NOESY peak volumes on the mixing time. Figure 14 shows the integrated peak volume for cross peaks joining the oleic acid methyl group (position 18) and the large group of unresolvable methylene groups (positions 4−7 and 12−17) to PEG as a function of mixing time. Intensities are normalized by the number of contributing hydrogen atoms. The data conform well to the approximate relation[26]

$$I = I_0 \sigma t_m \exp(-R t_m) \quad (1)$$

where I is the experimental cross-peak intensity, I_0 is an arbitrary scaling factor, σ is the cross-relaxation rate, t_m is the mixing time, and R is related to the relaxation rates of the interacting atoms. This expression can be linearized by dividing both sides by t_m and taking logarithms. A plot of $\ln(I/t_m)$ *vs* t_m gives an intercept of $\ln(I_0\sigma)$ and a slope of $-R$.

Cross-relaxation rates for all resolvable cross peaks with PEG were determined from linear regression analysis of linearized build-up curves for the sample described in Figure 14. The resulting relative cross relaxation rates are 74% (position 2), 95% (position 3), 100% (positions 4−7 and 12−17), 66% (positions 8 and 11), 48% (positions 9 and 10), and 28% (position 18). The values are normalized according to the number of protons contributing to each resolvable resonance frequency. The highest rate occurs for the large group of indistinguishable methylene protons found throughout the oleate molecule. Excluding these, the terminal methyl group and resolvable resonances near the double bond have smaller cross-relaxation rates than the resolvable resonances near the polar head group.

Discussion

With a few exceptions,[30] a decrease in the cmc value is often related to polymer−surfactant interactions and is used to monitor the interactions. However, for surfactant solutions with concentrations far above the cmc, and when detailed structural information is required, other methods are needed. Cryo-TEM provides images of aggregate structures and directly demonstrates their size and shape. Although cryo-TEM cannot detect individual polymer molecules, it can determine the effect on the surfactant aggregate structure of surfactant−polymer interactions. Rheometry provides information on macroscopic properties of the system, and provides microscopic information indirectly through the effects of structured aggregates on fluid flow. NMR is sensitive to molecular motions and can characterize polymer−surfactant interactions at the molecular level. Compared to cryo-TEM, NMR is less able to characterize aggregate shapes. Rheometry, electron microscopy, and NMR therefore provide complementary information. The combination of techniques can provide rich insight into the structure and dynamics of polymer−surfactant complexes and explain their function and their impact on physical properties of the solutions.

Surfactant solutions with globular micelles generally exhibit Newtonian behavior. The viscosity of the solution increases linearly with the volume fraction of the micelles according to Einstein's equation

$$\eta = \eta_s(1 + 2.5\phi) \quad (2)$$

where η_s is the viscosity of the pure solvent and ϕ is the effective volume fraction which takes into account the hydration of the molecules. Spherical micelles and short, threadlike micelles can fit this model. Water-soluble polymers, like PEG and PPG, also usually fit this model at the low concentrations used in the present work. However, when long, threadlike micelles form, entanglement of the micelles is known to give the solution viscoelastic character which cannot be explained by the

(30) Brackman, J. C.; van Os, N. M.; Engberts, J. B. F. N. *Langmuir* **1988**, *4*, 1266−1269.

Einstein model. When the entanglement breaks down (and micellar sizes decrease) as shown by cryo-TEM in this study, it is expected the solution will become Newtonian.

Cryo-TEM and NMR both support the conclusion that a consequence of the interaction of PEG with oleate micelles is a change in the micelles from long, threadlike structures to smaller aggregates. This structural transition underlies the large viscosity drop and the transition from a non-Newtonian to a Newtonian fluid. This transition is demonstrated directly by the cryo-TEM images which show a progressive decrease in micelle length as the polymer concentration is increased. NMR reflects this structural transition through the large increase in the diffusion coefficient of oleate caused by the presence of PEG. This demonstrates that the polymer is interacting with the surfactant aggregate, resulting in reduced aggregate size and increased surfactant mobility.

The effect of polymer molecular weight on the extent to which the aggregate size is reduced was also explored by NMR. The effect is small, with the oleate diffusion coefficients differing by only 8% in the presence of polymers differing in molecular weight by nearly a factor of 2. The observation that the polymer has a greater diffusion coefficient than the surfactant except at surfactant/polymer weight ratios of greater than 5:1 suggests that the polymer is not always bound to surfactant aggregates and a significant fraction is diffusing freely at a particular time. This is supported by the observation that for identical surfactant and polymer concentrations, the lower-molecular-weight polymer has a larger diffusion coefficient than the higher-molecular-weight polymer, even though the surfactant has roughly the same diffusion coefficient. This would be expected if the measured averaged diffusion coefficient were influenced by the larger diffusion coefficient of the unbound low-molecular-weight polymer compared to the unbound high-molecular-weight polymer. Since biphasic character in the polymer diffusion curves was not observed, the measured diffusion coefficients represent a weighted average and the rate of exchange is faster than the time scale of the diffusion measurements, approximately 100 ms.

Concentration- and temperature-dependent diffusion coefficients show that the surfactant−polymer aggregate size depends sensitively on these parameters. For the concentration-dependent diffusion data, if a single polymer-stabilized aggregate size were present, one would expect that the diffusion coefficient of the surfactant would be independent of polymer or surfactant concentration as long as sufficient polymer were present. Since the diffusion coefficients depend sensitively on concentrations of both components, it is likely that the aggregate sizes depend on concentrations, at least over the concentration ranges studied. The data do not address issues such as cross-linking of aggregates by polymers or the range of aggregate sizes. For the temperature-dependent diffusion data, the hydrodynamic radii change as a function of temperature. Temperature-dependent solution viscosity was accounted for in the calculations. Thus, average aggregate size also depends on temperature.

Quantitative interpretation of the NOESY cross peaks joining PEG with oleate resonances requires consideration of the factors controlling cross peak intensities. For a solution of identical, structurally well-defined systems, the intensity of NOESY cross peaks is related to the inverse sixth power of the distance between the corresponding atoms. The effect therefore falls off rapidly with distance and becomes negligible for distances >5 Å. In the present case, one expects several features of the system to complicate this simple relationship. For example, the system consists of a collection of different structures which may be interconverting rapidly or slowly within the experimental mixing time. Also, the time scales and relative importance of exchange, configurational interconversion, and aggregate tumbling are difficult to ascertain. Finally, for systems with long correlation times, spin diffusion is expected to be efficient. In the presence of spin diffusion, cross peaks between distant atoms have higher-than-expected intensity because intervening atoms can facilitate magnetization transfer. Since the effects of structural heterogeneity, configurational interconversion and exchange, and spin diffusion cannot be easily sorted out and analyzed, quantitative analysis of NOESY cross peak intensities is problematic for the present system.

Nonetheless, cross-relaxation is strongly biased toward short distances. The shortest distance of approach is given by the sum of van der Waals radii. Because of this distance dependence, only relatively closely neighboring atoms will give cross peaks. Averaging over all structures will give cross peaks whose intensities are very roughly proportional to the probability that two atoms are neighbors (≤ 5 Å) in the structure. Spin diffusion will have the effect of "flattening" the results, so that atoms which are mostly far away will appear to have a higher probability of being close. Differential dynamics will influence every cross peak differently. Assuming a single correlation time for the system will therefore introduce unpredictable errors throughout the system in a manner depending on the true dynamics of each interaction. If the correlation time is dominated by a uniform process such as aggregate tumbling, then this source of error is unimportant.

In view of these considerations, the cross-relaxation data show that all oleate atoms have some probability of being in close proximity to the PEG, or that spin-diffusion provides an efficient mechanism for transfer of magnetization throughout the aggregate. This result can be rationalized based on published molecular dynamics studies and by adopting the accepted "beads-on-a-string" model for surfactant/hydrophilic polymer interactions. Molecular dynamics calculations[31] on smaller spherical micellar systems suggest that surfactant atoms can be found anywhere within the micelle, though the distribution depends on the position in the chain. The "beads-on-a-string" model envisions polymer chains wrapped around micelle-like surfactant aggregates. Within these assumptions, the mixing time-dependence of the NOESY cross-peak intensities suggests that all surfactant atoms have some probability of being at the surface of the micelle in close proximity to the polymer found at the aggregate surface. Atoms near the polar end and unresolvable methylene groups have a higher probability of being at the surface than atoms at or near the double bond or terminal methyl group of the hydrophobic chain. The probabilities estimated from cross-peak build-up rates represent upper limits because of spin diffusion.

It has been demonstrated in some other surfactant systems, such as CTAB/NaSal,[16−18] and $C_{16}E_6$ and $C_{12}E_5$,[16] that a strong hydrophobic interaction between polymer and surfactant is necessary for the polymer-induced microstructural change to be appreciable. This means the hydrophobicity of either polymer or surfactant or both has to be large. As reflected in the ability of polymers PEG and PPG to reduce the size of oleate aggregates, the systems studied here showed the opposite tendency. Rheology, cryo-TEM, and NMR data all suggested that PEG is more effective in causing microstructural change in surfactant solution. Only spherical micelles were found

(31) Shelley, J.; Watanabe, K.; Klein, M. L. *Int. J. Quantum Chem.: Quantum Biol. Symp.* **1990**, *17*, 103−117.

in 1% PEG solution, whereas threadlike micelles were found in 1% PPG solution. Although the PEG used in the cryo-TEM study has higher molecular weight compared to PPG, molecular weight is not a likely cause of this effect. It has been widely accepted that for PEG, the molecular weight is not a factor in polymer−surfactant interaction if the molecular weight is between 4000 and 900 000.[32] It has also been found that PEG does not have appreciable interaction with CTAB micelles.[17] The NMR diffusion study also rules out effects of molecular weight because for solutions containing PEG-4600 or PEG-8000 at identical concentrations (by weight) of polymer and surfactant, the oleate diffusion coefficient is the same within 8%, indicating very similar aggregate structures.

This suggests that the hydrophobic interaction between polymer and surfactant molecules does not act as a dominant factor for polymer−surfactant interaction for the systems studied here. In this sense, oleate micelles interact differently than SDS micelles with PEG and PPG. PPG has a larger effect on SDS micelle size than PEG does,[21] as in the case of CTAB/NaSal micelles. The model by Nagarajan[13] does predict that PPG should bind more weakly than PEG because the former is less flexible and more bulky. It was argued that when CTAB micelles interact with PPG or PEG, because CTAB has a bulky head group, CTAB micelles can only accommodate less bulky PEG. That argument cannot explain the difference between the oleate and SDS micelles. On the other hand, the hydrophobicity of the polymer itself cannot explain our results either. This suggests that the interaction between PEG and oleate micelles is more complicated than the existing theories predict. The system certainly merits further study.

(32) Goddard, E. D. In *Interactions of Surfactants with Polymers and Proteins;* Goddard, E. D., Anathapadmanabham, K. P., Eds.; CRC Press: Boca Ratan, FL, 1993 pp 123−169.

Summary

This work demonstrates that addition of hydrophilic polymers to oleate solutions induces microstructural changes. The threadlike-to-spherical microstructure transition observed by cryo-TEM in oleate solution and the corresponding reduction in hydrodynamic radius observed by NMR correlate well with solution rheology changes. It was also found that the more hydrophilic polymer, PEG, is more effective than the more hydrophobic polymer, PPG, in inducing the threadlike-to-spherical microstructure transition. This differs from SDS/polymer and CTAB/polymer interactions, where more hydrophobic polymers are more effective. This result suggests that a hydrophobic interaction between polymer and surfactant molecules is not always a dominant or determining factor for forming polymer−surfactant complexes. Current models do not account for this result. NOESY spectra indicate either that all spectroscopically resolvable oleate hydrogen atoms have a measurable probability of residing in close proximity to the polymer or that spin diffusion provides an effective mechanism for transferring magnetization throughout the aggregate even at short mixing times. The sign of the NOESY cross peaks indicates that internal aggregate motions are in the spin-diffusion (slow) limit. The combination of rheology, cryo-TEM, and NMR provides a unique way to characterize polymer−surfactant interactions and to correlate microstructure with macroscopic solution properties.

Acknowledgment. Z. Lin thanks Mr. P. E. Cothran for his help in rheology measurements. The authors also thank John Shaffer and Lora Robosky for expert assistance with NMR measurements and sample preparation.

LA961004D